Hindawi Publishing Corporation
International Journal of Photoenergy
Volume 2014, Article ID 120693, 7 pages
http://dx.doi.org/10.1155/2014/120693

Research Article

An Alternative Approach for Improving Performance of Organic Photovoltaics by Light-Enhanced Annealing

En-Ping Yao, Chiu-Sheng Ho, Chang Yu, E-Ling Huang, Ying-Nan Lai, and Wei-Chou Hsu

Institute of Microelectronics, Department of Electrical Engineering, Advanced Optoelectronic Technology Center, National Cheng Kung University, No. 1, University Road, Tainan City 70101, Taiwan

Correspondence should be addressed to Wei-Chou Hsu; wchsu@eembox.ncku.edu.tw

Received 9 February 2014; Accepted 9 July 2014; Published 21 July 2014

Academic Editor: Serap Gunes

This work proposes an approach for improving the performance of poly(3-hexylthiophene) (P3HT-) based organic photovoltaics (OPVs). P3HT-based bulk heterojunction (BHJ) film can absorb the energy from 532 nm laser light and be transformed into favorable morphology. A combination of traditional thermal annealing and laser annealing improved device performance, with a slight increase in fill factor and a significant improvement in short-circuit current density. Better crystallization and a higher degree of molecular order in the thermal/laser coannealed P3HT-based BHJ film were observed through X-ray diffraction and Raman spectroscopy.

1. Introduction

Organic photovoltaics (OPVs) have attracted tremendous interest recently for renewable energy applications due to their low cost for large-area fabrication, light weight, and compatible processing on flexible substrates [1, 2]. Recently, poly(3-hexylthiophene) (P3HT) has been extensively studied due to its promising physical properties, including a high hole mobility of around 10^{-3} cm^2/Vs, a wide light absorption spectrum, and excellent environmental stability [3–6]. When P3HT is blended with fullerene derivatives, such as [6,6]-phenyl C_{61} butyric acid methyl ester (PCBM) [1] and indene-C_{60}-bisadduct (ICBA) [7], to build a bulk heterojunction (BHJ), it always plays a good role to mix with each fullerene derivative, which can lead to a fill factor (FF) of 65~72%.

BHJ should be a favorable structure for the light harvesting layer of OPVs. However, their morphology is thus very critical to OPV device performance. For P3HT-based BHJs, the morphology can be tuned via treatments such as solvent-vapor treatment [8–10], ultraviolet- (UV-) ozone exposure [11], microwave treatment [12, 13], pulsed-laser treatment [14], adding solvent additive [15–17], and thermal annealing treatment [18–21]. These methods efficiently change the morphology of P3HT-based BHJs and improve device performance. Thermal annealing treatment is most commonly applied to P3HT-based BHJs since it yields close-packed crystalline structures and strong interchain interactions [18–20].

Flexible substrates can be used for OPVs. However, long-term thermal annealing is challenging when building a device on a flexible substrate since the film may crack and become damaged due to the bending of the substrate. A method for transferring energy to the BHJ film and modifying its morphology without creating too much heat is thus desirable. Li et al. [21] applied a standard low-intensity fluorescent lamp to PCDTBT:PC_{60}BM blend film before thermal annealing and improved device lifetime and performance. Using a more exact wavelength of light that can be absorbed by the material will make the energy transfer process more efficient. P3HT has good absorption of light in the range of 500 to 560 nm. Therefore, P3HT will absorb the energy of light in this range shining on a P3HT-based BHJ film with sufficient power. In this work, a 532 nm green laser was used to irradiate P3HT:PCBM film at 50 mW as an annealing process to modify the film morphology. Thermal annealing only, laser annealing only, and thermal/laser coannealing treatments are compared.

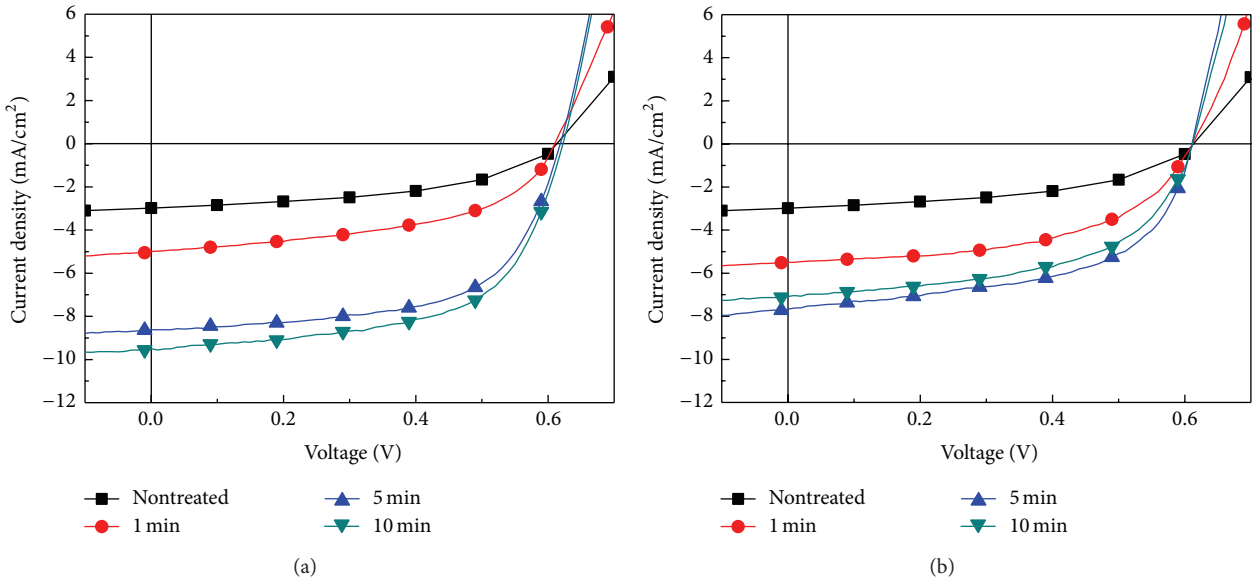

FIGURE 1: J-V characteristics of organic photovoltaic devices with (a) thermal annealing process and (b) laser annealing process under different duration.

2. Experimental Details

2.1. Device Fabrication. Indium tin oxide (ITO)-coated glass with a sheet resistance of 5 ohm/sq was utilized as the substrate of the OPV device. The substrates were sequentially cleaned in an ultrasonic bath with deionized water, acetone, and isopropanol, respectively, and then baked at 100°C for at least 1 h in an oven. The clean substrates were treated by O_2 plasma at 10 W for 1 min. Then, poly(3,4-ethylenedioxythiophene):poly(styrenesulfonate) (PEDOT:PSS), from H. C. Starck (CLEVIOS P VP AI4083), was spin-coated onto the ITO substrate at 4000 rpm (~35 nm) and then baked at 120°C for 15 min on a hot plate. The P3HT:PCBM, at a weight ratio of 1 : 1 and dissolved in 1,2-dichlorobenzene (DCB) solution with a concentration of 2 wt%, was spin-coated onto PEDOT:PSS at 800 rpm for 30 s (~200 nm). After the deposition of the P3HT:PCBM layer, the film was thermally annealed on a hot plate or irradiated with a 532 nm laser beam (diameter: 0.7 mm) at 50 mW or annealed on a hot plate and irradiated with a 532 nm laser beam simultaneously. After the P3HT:PCBM film had been thermally or laser annealed, LiF and Al were deposited at thicknesses of 1 and 100 nm, respectively, under a 3×10^{-6} Torr vacuum in a thermal evaporator. The device area was defined by a shadow mask to be 0.3×0.3 cm^2.

2.2. Device Measurement. The current density-voltage (J-V) characteristics of the OPV devices were measured by a Keithley 2400 source meter with an Oriel solar simulator system equipped with a xenon lamp and an AM 1.5G spectral filter. Additionally, the power conversion efficiency (PCE) of the solar cells was calculated using a Newport 91150V standard reference cell under a simulated light intensity of 100 mW/cm^2. The external quantum efficiency (EQE) was measured using an EQE measurement system (QE-3000, Titan Electro-Optics Co., Ltd.).

2.3. Film Characterization. The absorption spectrum was characterized using a JASCO UV-670/FP-6600 ultraviolet-visible (UV-vis) spectrophotometer. The X-ray diffraction (XRD) patterns were recorded by a Rigaku D/MAX2500 rotating-anode X-ray generator. Raman spectra were measured with a Renishaw Raman system.

3. Results and Discussion

3.1. J-V Characteristics of OPV Devices. Figure 1(a) shows the J-V characteristics of devices with P3HT:PCBM layer thermally annealed at 130°C for 0, 1, 5, and 10 min. The best device performance was obtained for the P3HT:PCBM film annealed for 10 min (more details can be found in our previous work [22]), with improvement in the short-circuit current density (J_{sc}) and FF. To compare laser annealing with thermal annealing, the J-V characteristics of devices subjected to 532-nm laser annealing at 50 mW for 0, 1, 5, and 10 min are shown in Figure 1(b). Details of the J-V characteristics of devices treated with thermal annealing and laser annealing for various durations are listed in Table 1. For the P3HT:PCBM film laser annealed for 1 min, the J_{sc} value of the device was nearly twice that obtained without annealing. The J_{sc} value further increased when the laser annealing time was increased to 5 min. However, a further increase to 10 min did not greatly affect device performance. The optimal laser annealing time is thus 5 min; however, the performance was not comparable to the device annealed by heat.

The J-V characteristics of devices with P3HT:PCBM film treated with thermal annealing and laser annealing simultaneously (thermal/laser coannealing) for various durations

Table 1: The V_{oc}, J_{sc}, FF, and PCE of the devices without annealing treatment, with thermal annealing process, and with laser annealing process under different duration.

Device treatment	Treated time (min)	V_{oc} (V)	J_{sc} (mA/cm^2)	FF	PCE (%)
Nontreated	—	0.61	3.11	0.49	0.93
Thermal annealing	1	0.61	4.99	0.52	1.58
	5	0.62	8.78	0.59	3.21
	10	0.62	9.52	0.60	3.54
Laser annealing	1	0.61	5.55	0.52	1.76
	5	0.61	7.38	0.52	2.34
	10	0.61	7.20	0.52	2.28

Table 2: The V_{oc}, J_{sc}, FF, and PCE of the devices with thermal/laser coannealing process under different duration.

Device treatment	Treated time (min)	V_{oc} (V)	J_{sc} (mA/cm^2)	FF	PCE (%)
Nontreated	—	0.61	3.11	0.49	0.93
Thermal and laser coannealing	1	0.61	6.83	0.53	2.21
	5	0.62	11.22	0.59	4.10
	10	0.62	10.55	0.60	3.92

are shown in Figure 2 and detailed in Table 2. Thermal/laser coannealed P3HT:PCBM film obtained better performance with the treating duration as 1, 5, and 10 min The significant enhancement in J_{sc} dominated the improvement of the device. A PCE of 4.10% was obtained with thermal/laser coannealing for 5 min. The PCE remained at around 4%, suggesting little change in morphology, when the coannealing time was further increased to 10 min. As a result, the thermal/laser coannealing process improved device performance compared to that obtained with thermal annealing only. Moreover, compared to the traditional thermal annealing process, the thermal/laser coannealing process requires half the time to obtain a given level of device performance.

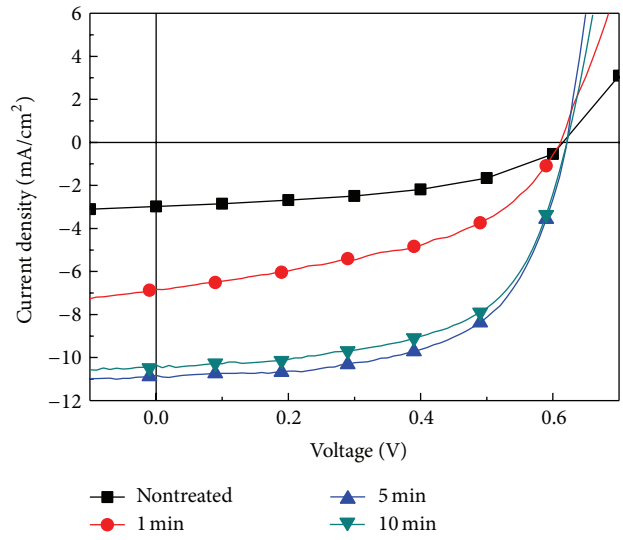

Figure 2: J-V characteristics of organic photovoltaic devices with thermal/laser coannealing process under different duration.

3.2. Absorption and EQE Spectra. Figure 3(a) shows the UV-vis absorption spectra of P3HT:PCBM films without annealing treatment, treated with thermal annealing only for 10 min and treated with thermal/laser coannealing for 5 min. There is a red shift for the films treated by thermal annealing only and thermal/laser coannealing compared to the unannealed film. The variation in the absorption spectrum may be due to the demixing of PCBM from P3HT, and thus an enhanced crystallinity of P3HT. Therefore, the interchain interactions among P3HT became stronger, leading to a longer conjugated length and a lower band gap between π and π^* orbitals [23]. Moreover, since the number of photons absorbed from the light corresponds to the current produced from the light harvesting layer, the intensity of the absorption spectrum could simply indicate the improvement in the J_{sc} value of the devices, as shown above. Figure 3(b) shows the EQE of the devices with P3HT:PCBM films without any treatment, treated with thermal annealing only for 10 min and treated with thermal/laser coannealing for 5 min. A significant enhancement in EQE can be observed after annealing treatment. The EQE of the film treated with thermal/laser coannealing for 5 min is higher than that of the film treated with thermal annealing only for 10 min which matches the improvement on J_{sc} of the devices as shown above. Hence, after adding laser treatment under thermal annealing process, the absorption ability of P3HT:PCBM film was enhanced resulting in higher J_{sc} of the device which declared that more favorable morphology was derived.

3.3. XRD Analysis. To investigate the morphological difference between P3HT:PCBM films, XRD was used to estimate the crystallinity of P3HT in the films. Figure 4 shows the XRD patterns of P3HT:PCBM films without any treatment, treated with thermal annealing only for 10 min and treated with

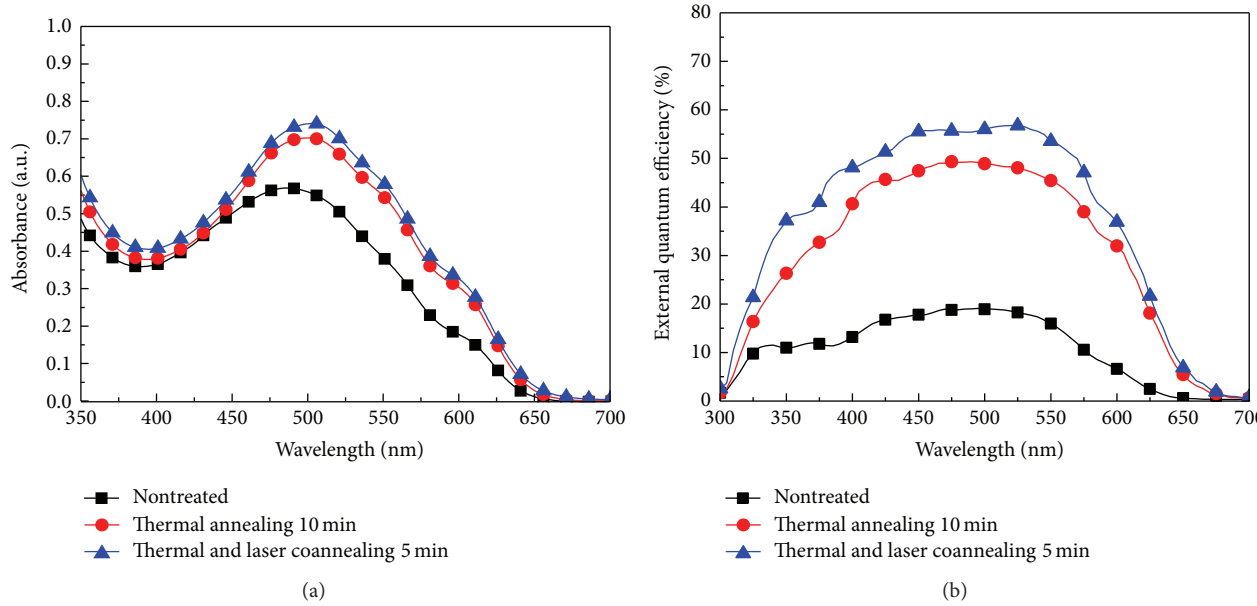

Figure 3: The (a) UV-vis absorption spectrum of P3HT:PCBM films and (b) the external quantum efficiency of the devices under different annealing process.

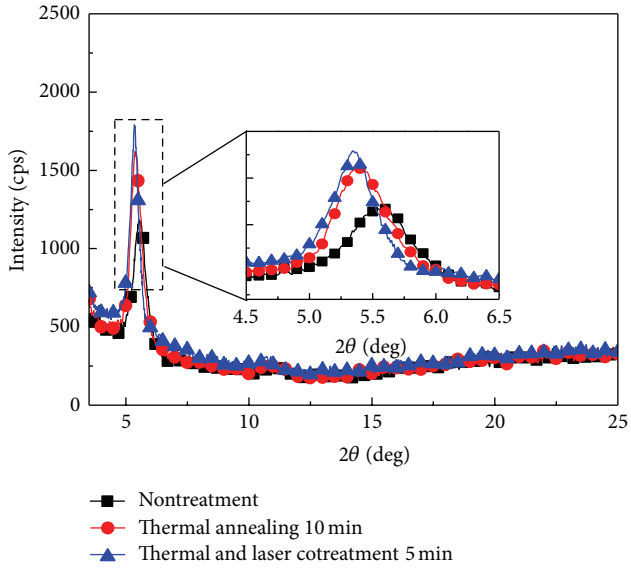

Figure 4: XRD spectra of P3HT:PCBM films under different annealing process. The insets show the zoomed-in graph of XRD spectra with the range from $2\theta = 4.5^\circ$ to $2\theta = 6.5^\circ$.

thermal/laser coannealing for 5 min. Obvious diffraction peaks appear at $2\theta = 5.58^\circ$, 5.39°, and 5.38° for each film. These peaks originate from polymer crystallites of the (100) orientation (backbone parallel and side-chains perpendicular to the substrate) [24–26]. The corresponding lattice constant d can be calculated using Bragg's law as

$$n\lambda = 2d \sin\theta, \quad (1)$$

where λ (=0.154056 nm) is the wavelength of the incident beam, 2θ is the angle between the incident and scattered X-ray wave vectors, and n is the interference order. The lattice constant d of the films without any treatment, treated with thermal annealing only for 10 min and treated with thermal/laser coannealing for 5 min, was calculated as 1.58, 1.63, and 1.64 nm, respectively. A higher lattice constant corresponds to a larger grain boundary of crystallization, which means that the grain boundary of crystal P3HT was similarly enlarged with thermal annealing only and thermal/laser coannealing. Moreover, the intensity of the peak is correlated with the crystallinity of P3HT. Therefore, annealing with heat and a laser simultaneously leads to better crystallinity of P3HT than that obtained with heat only. Combining laser and thermal annealing promotes the formation of crystalline P3HT domains and enhances carrier transport due to more resonance of π-electrons in the polymer chain [27–30]. Li et al. [21] found that most of the contribution from light annealing (through a fluorescent lamp) is related to the formation of PCBM clusters in the BHJ layer. However, in this work, the laser light was mainly absorbed by P3HT since its wavelength matches the absorbance of P3HT but not PCBM. Therefore, the crystallinity of P3HT chains dominates the variation of the morphology of the BHJ film, as shown in the XRD analysis.

3.4. AFM Phase Analysis. The morphological variation of P3HT:PCBM films treated with various annealing processes was analyzed using atomic force microscopy (AFM) phase images, as shown in Figure 5. Figure 5(a) shows that there is no obvious phase separation on the surface of the P3HT:PCBM film without any annealing treatment. For the P3HT:PCBM film treated with thermal annealing only for

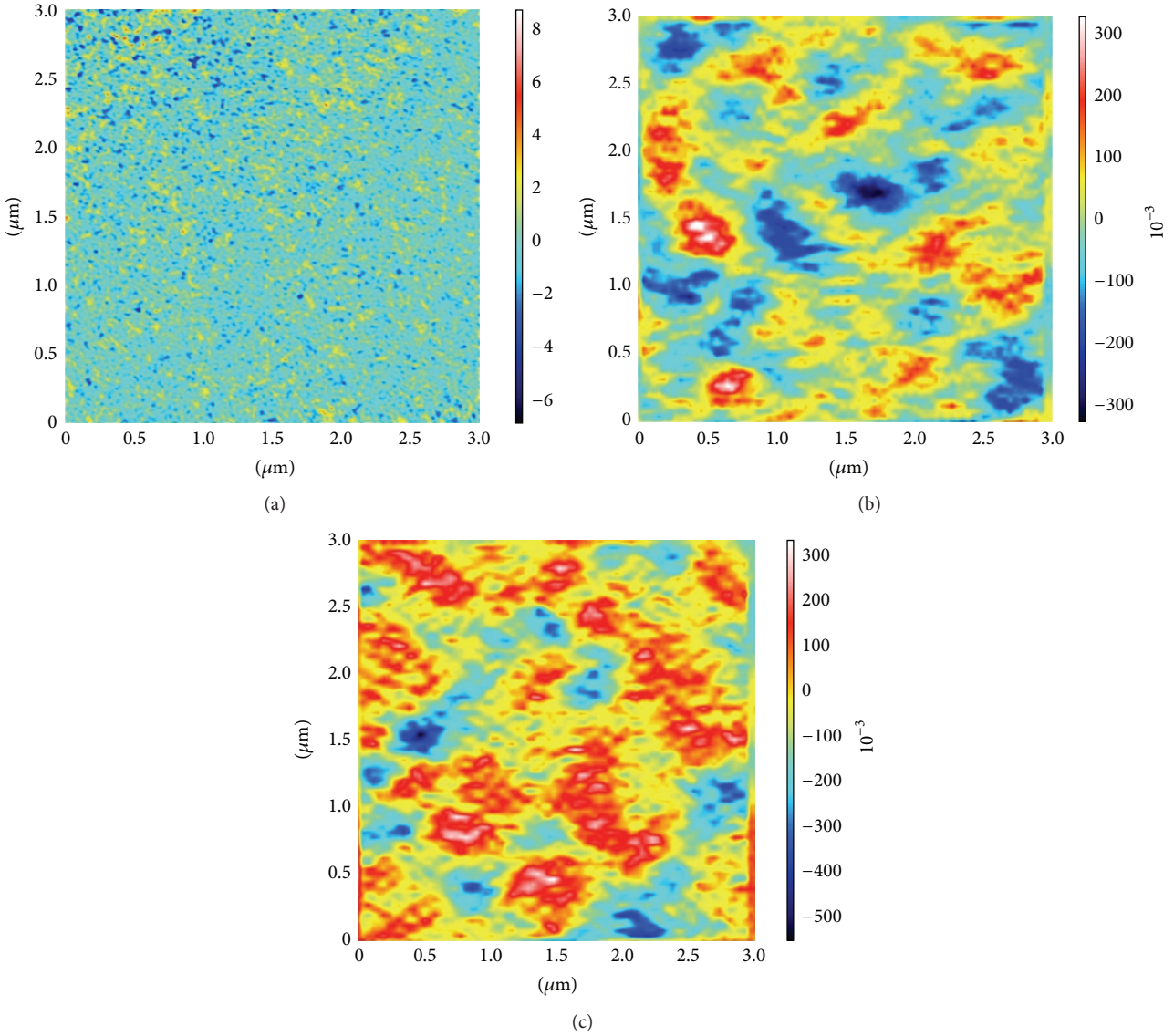

Figure 5: AFM phase images of P3HT:PCBM films (a) without annealing treatment, (b) with thermal annealing for 10 min, and (c) with laser/thermal coannealing for 5 min.

10 min (Figure 5(b)), significant phase separation with large grain sizes can be observed, which indicates that thermal annealing results in better crystallization of P3HT chains. Moreover, the phase image of the film treated with thermal/laser coannealing for 5 min (Figure 5(c)) shows even more phase separation and larger grain sizes, indicating much better crystallization of P3HT chains. The AFM phase analysis shows a great variation in the morphology of P3HT:PCBM films treated with various annealing processes, which supports the XRD analysis. These results confirm that thermal annealing changes the morphology of P3HT:PCBM film and improves device performance. Introducing laser light into the annealing process makes the morphology of P3HT:PCBM film more favorable and leads to better PCE.

3.5. Raman Analysis. Figure 6 shows the normalized Raman spectra of P3HT:PCBM films without any treatment, treated with thermal annealing only for 10 min and treated with thermal/laser coannealing for 5 min under 514 nm resonant excitation. The main in-plane ring skeleton modes at ~1445 cm^{-1} (symmetric C=C stretch mode) and ~1381 cm^{-1} (C–C intraring stretch mode), the interring C–C stretch mode at ~1208 cm^{-1}, the C–H bending mode with the C–C interring stretch mode at ~1180 cm^{-1}, and the C–S–C deformation mode at 728 cm^{-1} appear. Among these Raman modes, this study focused on the two main in-plane ring skeleton modes at ~1445 and ~1381 cm^{-1}, as they are supposed to be sensitive to the π-electron delocalization (conjugation length) of P3HT molecules [30, 31]. In Figure 6, compared to the P3HT:PCBM film without any treatment, the Raman peak of the C=C symmetric stretch mode shifted to a lower wavenumber, from 1455 cm^{-1} to 1453 cm^{-1}, for the film treated with thermal annealing for 10 min, and an even lower wavenumber, from 1455 cm^{-1} to 1450 cm^{-1}, and for the film treated with thermal/laser coannealing for 5 min. The

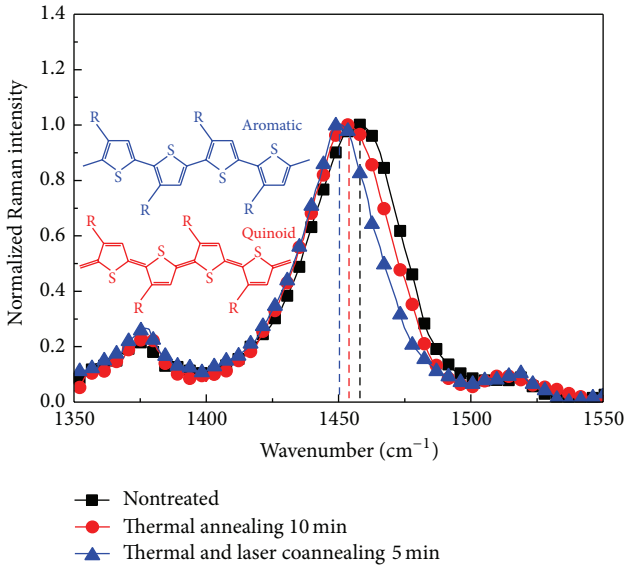

Figure 6: Normalized Raman spectrum wave numbers (C=C and C–C modes) of P3HT:PCBM films under different annealing process. The inset shows the aromatic form and quinoid form of the P3HT interchain.

decrease in the wavenumber of the peak position indicates that the aromatic form of polymer rings transformed into the quinoid form [31], as shown in the inset in Figure 6. With more quinoid form polymer rings, more delocalized conjugated π-electrons were obtained, which enhanced charge transfer. The full width at half maximum (FWHM) of this C=C mode for the P3HT:PCBM film annealed by heat only (35 cm^{-1}) is smaller than that of the film without any treatment (39 cm^{-1}), reflecting the higher degree of molecular order of the former. Moreover, the FWHM of the film treated with thermal/laser coannealing (34 cm^{-1}) was slightly smaller than that of the film treated by thermal annealing only, implying a better molecular order. A more favorable morphology of P3HT:PCBM film was thus obtained with thermal/laser coannealing, which led to better absorbance and charge transfer of the BHJ and improved J_{sc} of the device.

4. Conclusion

This study proposed an annealing method that combines laser annealing and thermal annealing and applied it to P3HT:PCBM films. P3HT:PCBM films treated with thermal/laser coannealing had a more favorable morphology and better carrier transport than those of the film treated with thermal annealing only. The better carrier transport in the BHJ layer led to higher J_{sc} and FF values and improved the device PCE. Since the devices are improved with less heat, the process is suitable for fabricating devices on flexible substrates.

Conflict of Interests

The authors declare that there is no conflict of interests regarding the publication of this paper.

Acknowledgment

This work was supported by the National Science Council of China, Taiwan, under Grant nos. NSC 100-2221-E-006-041-MY3 and NSC 101-3113-E-006-014-.

References

[1] G. Li, V. Shrotriya, J. Huang et al., "High-efficiency solution processable polymer photovoltaic cells by self-organization of polymer blends," *Nature Materials*, vol. 4, no. 11, pp. 864–868, 2005.

[2] W. Ma, C. Yang, X. Gong, K. Lee, and A. J. Heeger, "Thermally stable, efficient polymer solar cells with nanoscale control of the interpenetrating network morphology," *Advanced Functional Materials*, vol. 15, no. 10, pp. 1617–1622, 2005.

[3] C. W. Chu, H. Yang, W. J. Hou, J. Huang, G. Li, and Y. Yang, "Control of the nanoscale crystallinity and phase separation in polymer solar cells," *Applied Physics Letters*, vol. 92, no. 10, Article ID 103306, 2008.

[4] V. D. Mihailetchi, H. Xie, B. de Boer et al., "Origin of the enhanced performance in poly(3-hexylthiophene): [6, 6]-phenyl acid methyl ester solar cells upon slow drying of the active layer," *Applied Physics Letters*, vol. 89, no. 1, Article ID 012107, 2006.

[5] X. Yang, J. Loos, S. C. Veenstra et al., "Nanoscale morphology of high-performance polymer solar cells," *Nano Letters*, vol. 5, no. 4, pp. 579–583, 2005.

[6] D. Chirvase, J. Parisi, J. C. Hummelen, and V. Dyakonov, "Influence of nanomorphology on the photovoltaic action of polymer-fullerene composites," *Nanotechnology*, vol. 15, no. 9, pp. 1317–1323, 2004.

[7] Y. He, H. Y. Chen, J. Hou, and Y. Li, "Indene—C_{60} bisadduct: a new acceptor for high-performance polymer solar cells," *Journal of the American Chemical Society*, vol. 132, no. 4, pp. 1377–1382, 2010.

[8] Y. Zhao, X. Guo, Z. Xie, Y. Qu, Y. Geng, and L. Wang, "Solvent vapor-induced self assembly and its influence on optoelectronic conversion of poly(3-nexylthiophene): methanofullerene bulk heterojunction photovoltaic cells," *Journal of Applied Polymer Science*, vol. 111, no. 4, pp. 1799–1804, 2009.

[9] E. Verploegen, C. E. Miller, K. Schmidt, Z. Bao, and M. F. Toney, "Manipulating the morphology of P3HT-PCBM bulk heterojunction blends with solvent vapor annealing," *Chemistry of Materials*, vol. 24, no. 20, pp. 3923–3931, 2012.

[10] S. Miller, G. Fanchini, Y. Lin et al., "Investigation of nanoscale morphological changes in organic photovoltaics during solvent vapor annealing," *Journal of Materials Chemistry*, vol. 18, no. 3, pp. 306–312, 2008.

[11] T. Hu, F. Zhang, Z. Xu, S. Zhao, X. Yue, and G. Yuan, "Effect of UV-ozone treatment on ITO and post-annealing on the performance of organic solar cells," *Synthetic Metals*, vol. 159, no. 7-8, pp. 754–756, 2009.

[12] H. Flügge, H. Schmidt, T. Riedl et al., "Microwave annealing of polymer solar cells with various transparent anode materials," *Applied Physics Letters*, vol. 97, no. 12, Article ID 123306, 2010.

[13] C. Ko, Y. Lin, and F. Chen, "Microwave annealing of polymer photovoltaic devices," *Advanced Materials*, vol. 19, no. 21, pp. 3520–3523, 2007.

[14] E. W. Okraku, M. C. Gupta, and K. D. Wright, "Pulsed laser annealing of P3HT/PCBM organic solar cells," *Solar Energy Materials and Solar Cells*, vol. 94, no. 12, pp. 2013–2017, 2010.

[15] L. Chang, H. W. A. Lademann, J. Bonekamp, K. Meerholz, and A. J. Moulé, "Effect of trace solvent on the morphology of P3HT:PCBM bulk heterojunction solar cells," *Advanced Functional Materials*, vol. 21, no. 10, pp. 1779–1787, 2011.

[16] D. M. Lyons, R. J. Ono, C. W. Bielawski, and J. L. Sessler, "Porphyrin-oligothiophene conjugates as additives for P3HT/PCBM solar cells," *Journal of Materials Chemistry*, vol. 22, no. 36, pp. 18956–18960, 2012.

[17] B. Peng, X. Guo, Y. Zou, C. Pan, and Y. Li, "Performance improvement of annealing-free P3HT: PCBM-based polymer solar cells via 3-methylthiophene additive," *Journal of Physics D: Applied Physics*, vol. 44, no. 36, Article ID 365101, 2011.

[18] M. Al-Ibrahim, O. Ambacher, S. Sensfuss, and G. Gobsch, "Effects of solvent and annealing on the improved performance of solar cells based on poly(3-hexylthiophene): fullerene," *Applied Physics Letters*, vol. 86, no. 20, Article ID 201120, pp. 1–3, 2005.

[19] Y. Kim, S. A. Choulis, J. Nelson, D. D. C. Bradley, S. Cook, and J. R. Durrant, "Device annealing effect in organic solar cells with blends of regioregular poly(3-hexylthiophene) and soluble fullerene," *Applied Physics Letters*, vol. 86, Article ID 063502, 2005.

[20] M. Reyes-Reyes, K. Kim, and D. L. Carroll, "High-efficiency photovoltaic devices based on annealed poly(3-hexylthiophene) and 1-(3-methoxycarbonyl)-propyl-1- phenyl-(6,6) C61 blends," *Applied Physics Letters*, vol. 87, no. 8, Article ID 083506, 2005.

[21] Z. Li, H. C. Wong, Z. Huang et al., "Performance enhancement of fullerene-based solar cells by light processing," *Nature Communications*, vol. 4, article 3227, 2013.

[22] C. S. Ho, E.-L. Huang, W. C. Hsu et al., "Thermal effect on polymer solar cells with active layer concentrations of 3–5 wt %," *Synthetic Metals*, vol. 162, no. 13-14, pp. 1164–1168, 2012.

[23] G. Li, V. Shrotriya, Y. Yao, and Y. Yang, "Investigation of annealing effects and film thickness dependence of polymer solar cells based on poly(3-hexylthiophene)," *Journal of Applied Physics*, vol. 98, no. 4, Article ID 043704, 2005.

[24] T. J. Prosa, M. J. Winokur, J. Moulton, P. Smith, and A. J. Heeger, "X-ray structural studies of poly(3-alkylthiophenes): an example of an inverse comb," *Macromolecules*, vol. 25, no. 17, pp. 4364–4372, 1992.

[25] K. E. Aasmundtveit, E. J. Samuelsen, M. Guldstein et al., "Structural anisotropy of poly(alkylthiophene) films," *Macromolecules*, vol. 33, no. 8, pp. 3120–3127, 2000.

[26] T. Erb, S. Raleva, U. Zhokhavets et al., "Structural and optical properties of both pure poly(3-octylthiophene) (P3OT) and P3OT/fullerene films," *Thin Solid Films*, vol. 450, no. 1, pp. 97–100, 2004.

[27] T. Erb, U. Zhokhavets, G. Gobsch et al., "Correlation between structural and optical properties of composite polymer/fullerene films for organic solar cells," *Advanced Functional Materials*, vol. 15, no. 7, pp. 1193–1196, 2005.

[28] C. Y. Yang, C. Soci, D. Moses, and A. J. Heeger, "Aligned rrP3HT film: structural order and transport properties," *Synthetic Metals*, vol. 155, no. 3, pp. 639–642, 2005.

[29] K. Kanai, T. Miyazaki, H. Suzuki, M. Inaba, Y. Ouchi, and K. Seki, "Effect of annealing on the electronic structure of poly(3-hexylthiophene) thin film," *Physical Chemistry Chemical Physics*, vol. 12, pp. 273–282, 2010.

[30] M. Cardona and G. Güntherodt, *Light Scattering in Solids VI*, vol. 68, Springer, Berlin, Germany, 1991.

[31] Y. Gao and J. K. Grey, "Resonance chemical imaging of polythiophene/fullerene photovoltaic thin films: Mapping morphology-dependent aggregated and unaggregated C=C species," *Journal of the American Chemical Society*, vol. 131, no. 28, pp. 9654–9662, 2009.